



## **Reconnaissance of Combined Punching Shear with Flexure in RC Slabs with Different Boundary Conditions**

Emad El-Din Ogail<sup>1</sup>, Ahmed Baraghith<sup>2</sup>, Salah El-Din Taher<sup>3</sup>, Tarek El-Shafiey<sup>4</sup>

<sup>1</sup> Demonstrator, Faculty of Engineering, Tanta University

E-mail: [emad.ogail@f-eng.tanta.edu.eg](mailto:emad.ogail@f-eng.tanta.edu.eg)

<sup>2</sup> Assistant professor, Faculty of Engineering, Tanta University.

E-mail: [ahmed.baraghit@f-eng.tanta.edu.eg](mailto:ahmed.baraghit@f-eng.tanta.edu.eg)

<sup>3</sup> Professor of concrete structures, Faculty of Engineering, Tanta University

E-mail: [salah.taher@f-eng.tanta.edu.eg](mailto:salah.taher@f-eng.tanta.edu.eg)

<sup>3</sup> Professor of concrete structures, Faculty of Engineering, Tanta University

E-mail: [tarek.elshafiey@f-eng.tanta.edu.eg](mailto:tarek.elshafiey@f-eng.tanta.edu.eg)

### **ABSTRACT**

Many of the previous researchers dealt with punching mechanism as a local failure of two-way action in slabs. Focus was devoted to flat slabs exhibiting rigid body separation of punched zone. Unbalanced moment was an important parameter especially for exterior and corner columns. However, limited attention was directed to interaction of flexure and punching of slabs with different boundary conditions. This situation is typical for small patch loads of truck wheel print on roadway girders. In this paper, a brief summary is presented to capture the fundamental aspects in the literature. Experimental program has been conducted for 1700x1700x120 mm RC slabs made of high performance concrete. Five specimens were centrally loaded with 150x150 mm patch under monotonic quasi-static force up to failure. The boundary condition simulated: (1) simply supported along two parallel sides, (2) simply supported along three sides, (3) simply supported along four sides, (4) simply supported along two adjacent sides and opposite corner support and (5) on four corner supports. Moreover, nonlinear finite element analysis was carried out to model the case studies and to conduct parametric investigation regarding the effect of tensile reinforcement ratio, the presence of compression steel mesh of partial or full span, the influence of concrete grade and the size of the slab to account for different combination of punching shear and flexural moment. Finally, analytical formulas and code equations were examined for the considered cases.

**Keywords:** RC slabs, punching shear, flexure, nonlinear finite element analysis, international codes, numerical simulation.

## INTRODUCTION

Most of the researches on punching phenomenon highlighted occurrence of two way shear in the vicinity of the loaded area [1-35]. Although a great effort was devoted to understand and manipulate fundamental parameters related to flat slabs and unbalanced moment transfer from slab to column [1]. However, many typical situations exist for girder type systems where boundary conditions differ from flat slabs [2]. Examples are shown in Fig. (1) for two failure cases in Egypt and Japan [3]. There still exists scarcity of data related to the effect of bending moment (balanced moment) at the punching zone on the two way mechanism of local failure. Boundary condition and size effect along with load location within the slab need to be further considered.



a. Punching test in Japan by Ngo [3]



b. Al. Morashaha bridge, Tanta (2016).

**Fig. 1: Failure case of bridge decks by punching.**

Elsanadedy et al. [36] conducted an extensive comparison between some of the international codes and well-reported experimental data. It was significant that considerable variation in the approaches used to assess shear resistance in punching. For example, the critical section is specified at distances between 0.5 to 2.0 times the effective depth ( $d$ ) from the loaded area. The root of concrete strength which contributes to the concrete punching shear resistance is taken equal to  $1/2$  in ECP 203-07 [37] and ACI 318-14 [38] while  $1/3$  in the European codes [39, 41]. The influence of flexure reinforcement, which has a significant effect based on the experimental tests [18] was considered only in BS 8110-97 [41]. Analytical formulas do not have a term to calculate the influence of size effect but CSA-A23.3-04 [40] formula took account for size effect of slabs thicker only than 300 mm. On the other hand, EC2-2004 [39] and BS8110-97 [41] considered the influence of flexure reinforcement and size effect for all slabs

Table (1) summarizes the main parameters considered experimentally in previous work that affect the punching characteristics. Limited attention was paid to correlate the applied bending moment to the punching capacity. This motivated to conduct the present research in order to capture the salient features acquainted to the problem. The methodology followed in the manuscript is to elaborate the exploration experimental program than demonstrate the parametric study using nonlinear finite element analysis. Finally, a formula to incorporate the influencing parameters is proposed to modify the Egyptian code equation and validity the process against many well-reported experimental data.

Table 1: Summary of main parameters considered experimentally for punching.

Parameters			Effect of the parameter
Reinforcement	Tension Reinforcement	Ratio	Increasing the ratio of tension reinforcement enhances the punching shear capacity and decrease ductility. [21]
		Distribution	The effective width recommended which the flexure reinforcement will contribute is to be taken three times of depth around the face of support. [20]
	Compression Reinforcement	Ratio	Compression reinforcement has little effect in increasing the ultimate load.[5, 18]
		Post punching behavior	<ul style="list-style-type: none"> <li>- Compression reinforcement improves the post punching behavior and can increase the residual strength of the slabs. [4]</li> <li>- Compression reinforcement acts as a suspension net supplying an alternate load path that holds the slab together even after failure. [17]</li> </ul>
Shear Reinforcement	Stirrups, shearhead reinforcement, shear bolts and studs	Enhancement of shear capacity is achieved [13, 41]	
Materials	Compressive strength of concrete	Proportionality correlation	<ul style="list-style-type: none"> <li>- Brittleness of high strength concrete reduces the rate of punching increase of punching strength with increasing concrete grade [8, 16].</li> <li>- Punching shear strength is enhanced by increasing the compressive strength of concrete. [36]</li> </ul>
	Fiber inclusion	<ul style="list-style-type: none"> <li>-Fiber type: steel, glass or polypropylene.</li> <li>- Volume fraction</li> </ul>	<ul style="list-style-type: none"> <li>- Post-punching is affected by presence of fiber [44]</li> </ul>
Geometry	Size effect	Slab length and thickness	Increasing the span induces higher bending moment and therefore manifests cracking of the punching zone and reduces the resistances [22, 33]
	Patch dimension	Side length of the loaded area	- Increasing the ratio of the column dimension to the depth of slab lead to decrease the shear strength. [30,41]
Restraining Effects	Membrane forces	Axial loading and in-plane stretching	<ul style="list-style-type: none"> <li>- Punching shear capacity is enhanced by the rotational restraint applied at the edges of slabs. [34]</li> <li>- Crack width and deflection are smaller than in the simply supported slabs. [40]</li> </ul>
Load Location and patch size	Concentrated load effect	Influence of support constraint	Punching shear capacity is increased as the concentrated load move towards the supports. [2]

## EXPERIMENTAL PROGRAM

The experimental program comprised five square specimens cast with concrete of target grade of 60MPa. The cubic meter of the mix consisted of 450 Kg Ordinary Portland Cement, 1279 Kg basalt of nominal size 10mm, 535 Kg siliceous sand, 45 Kg silica fume, 4.5L high range superplasticizer and water/binder ratio of 0.3. Table (2) lists the tested groups under different boundary conditions. The patch size was 150mm square plate of 40mm thickness. Fig. (2) illustrates the test set-up and the instrumentation. Digital data acquisition system connected to a computerized storage measured the load cell, strain gages and LVDTs readings.

Table 2: Data of experimental specimens.

Restraint Designation	Experiment Specimen	Dimensions			Concrete grade $f_{cu}$ , MPa	Bottom steel mesh	Boundary conditions
		L (mm)	t (mm)	$d_{avg}$ (mm)			
G0	G00	1700	120	100	72	T16 @ 120 mm	Simply supported on two opposite sides
G1	G10	1700	120	100	58	T16 @ 120 mm	Simply supported on four sides
G2	G20	1700	120	100	67	T16 @ 120 mm	Simply supported on three sides and the 4 <sup>th</sup> is free
G3	G30	1700	120	100	64	T16 @ 120 mm	Simply supported on two adjacent sides and pin support on the opposite corner
G4	G40	1700	120	100	62	T16 @ 120 mm	Pin supports on four corners



Fig. 2: Experimental set-up and instrumentation.

Specimen G00 provided actual data about the one-way action and the nominal flexural capacity of the specimens. Fig. (3) depicts the bottom views of the slabs after the onset of punching shear in slabs possessing two way action. Of course, flexural cracks existed in all specimens as central loading was applied but finally the localized punching occurred. Radial and circumferential cracks underneath the patch load were observed but with relatively different configurations. Boundary conditions influenced the final punching shape as well as the load deflection relationship as shown in Fig. (4). Imposing more support constraint markedly affected the peak load and the brittleness of the response. In the absence of punching phenomenon, specimen G00 provided the highest failure load and longest peak plateau due to flexural ductility of the under reinforced sectional behavior. Increasing the length of the unsupported perimeter as in G40, then G30 followed by G20 affected the system stiffness and hence resulted in higher deflection at the peak load. The least deflection at the onset of punching was expectedly monitored for specimen G10 which was simply supported on the four sides. Presence of the short polypropylene fibers maintained the integrity of the failed specimens and induced post-punching residual capacity that may be noticed in the load-central deflection relationship prior to final failure. In all punching mechanisms, top penetration took place very close to the peak load then abrupt load capacity occurred. Continuous tearing of fibers bridging cracks was heard with the progress of loading after cracking. Such crack bridging by fibers augmented post-peak survival and enhanced the toughness per se.

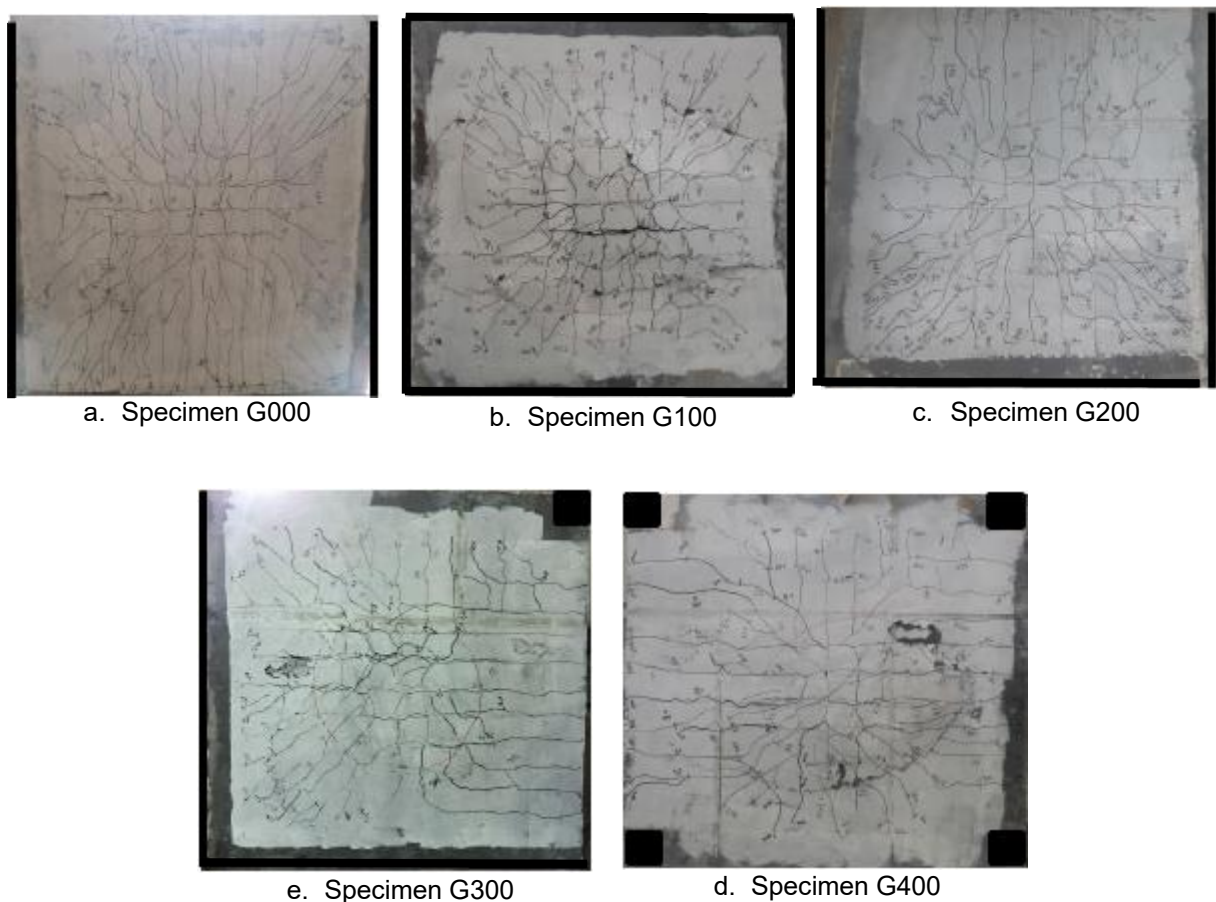


Fig. 3: Failure patterns of the tested specimens.

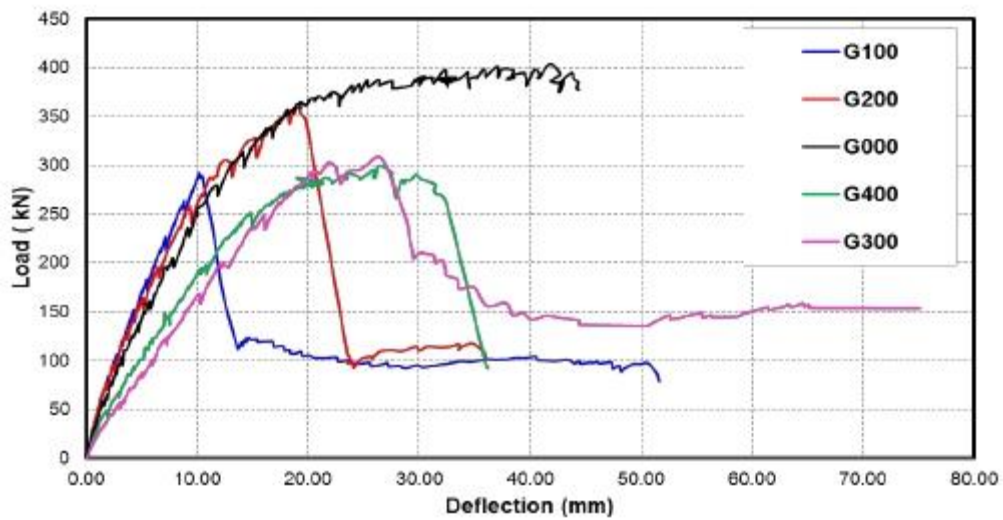


Fig. 4: Load–central deflection diagrams of tested specimens.

### NON-LINEAR FINITE ELEMENT SIMULATION

The finite element simulation has been carried out by two models. The first model used shell elements to predict the moment and shear with the progress of loading. Fig. (5) demonstrates the maximum bending moments at the peak load. It is clear that the moment contour surfaces were drastically affected by the boundary conditions.

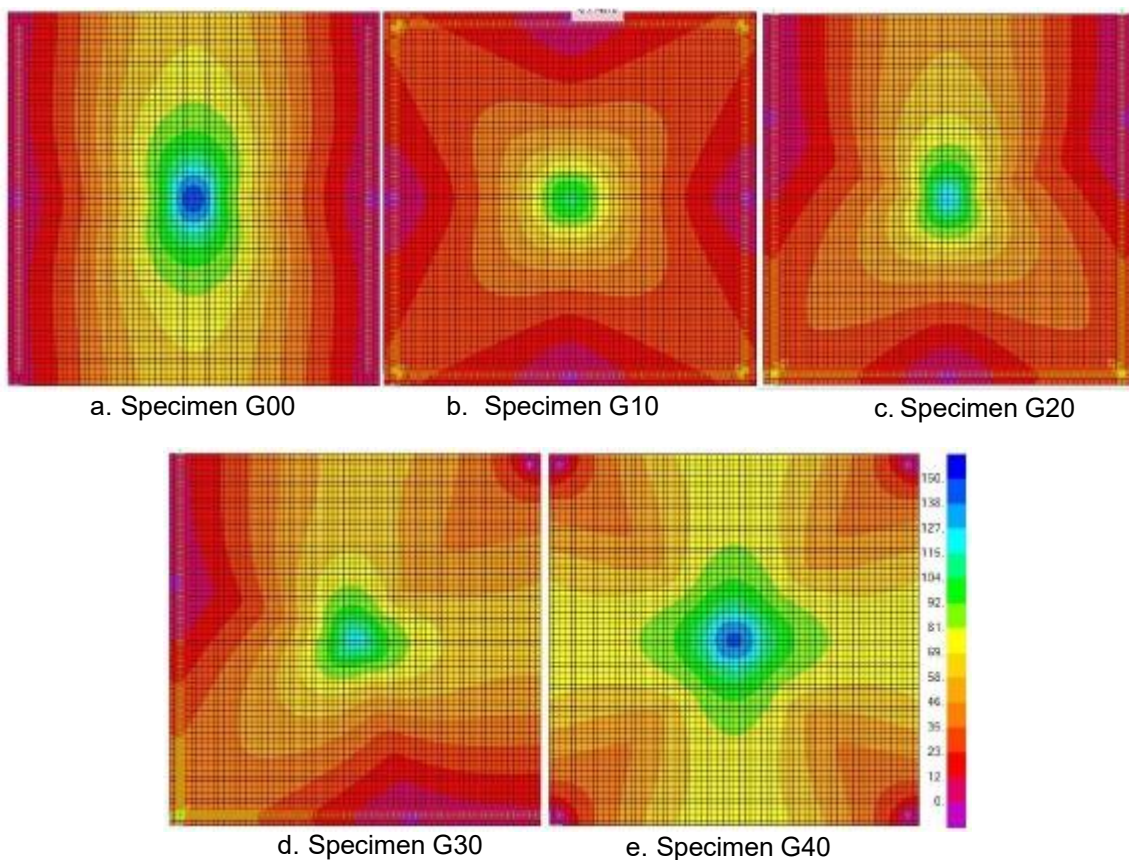


Fig. 5: Bending moment contours of tested specimens.

The other finite element (FE) model, shown in Fig. (5), was made by ANSYS 15 using three-dimensional brick elements for concrete of grade 60 MPa with smeared distribution of the fibers in all case studies. Steel reinforcement was idealized by link elements and thus dowel action was not considered. Trying to properly simulate the experimental support conditions, frictional elements were used for the simply supported restraints thus allowing horizontal movement governed by the concrete-steel plate friction and the exhibited vertical reaction. Moreover, the simulation does not prevent uplift or rotation wherever takes place. The incentive of this modeling was to view the within thickness formation and propagation of cracks and crushing of concrete with various stages of loading. Keeping in mind that there was difference of the concrete grade, Table (3) demonstrates the close agreement of the experimental versus the finite element simulation.

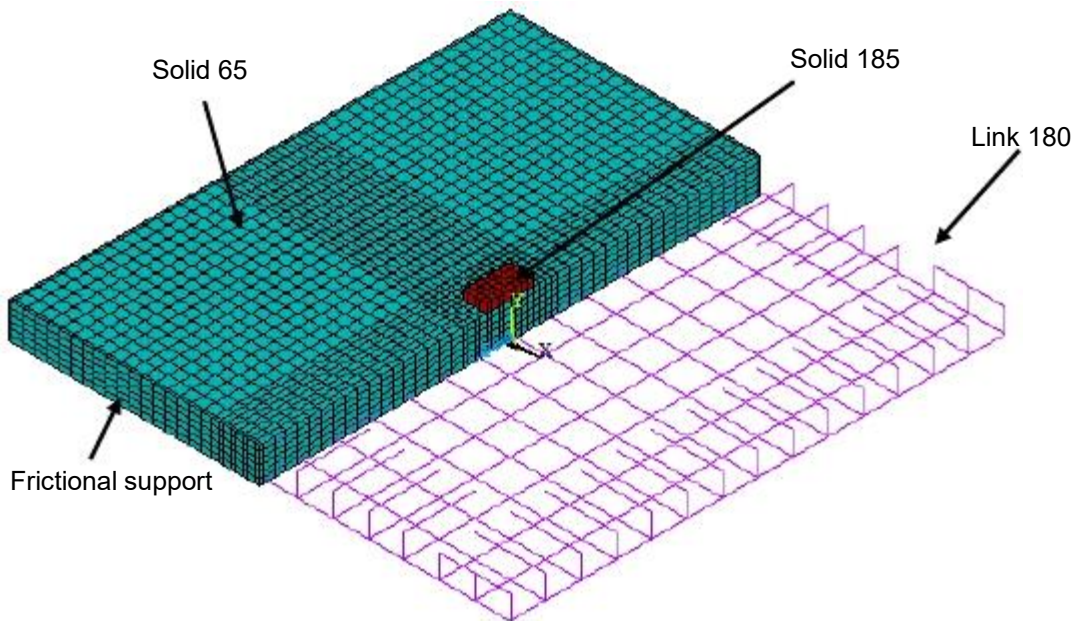


Fig. 5: Finite element mesh of the problem (3-D solid element discretization.)

Table 3: The ultimate punching load of the simulation against the experiments.

Specimens	Finite Element Prediction		Experimental		Ratio	
	$V_{cr,FE}$ (kN)	$V_{u,FE}$ (kN)	$V_{cr,EXP}$ (kN)	$V_{u,EXP}$ (kN)	$\frac{V_{cr,EXP}}{V_{cr,FE}}$	$\frac{V_{u,EXP}}{V_{u,FE}}$
G10	87	311	75	291	0.862	0.935
G20	86	320	89	358	1.035	1.118
G30	84	319	73	307	0.869	0.962
G40	81	305	74	297	0.914	0.973

Discarding the post-peak regime, Fig. (6) illustrates the close agreement of the finite element predictions with the experimental curves. However, the cracking effect on the tangent stiffness is more obvious in the finite element simulation. It has to be pointed out that the experimental determination of the cracking load is based mainly on the visual inspection using optical micrometer rather than estimating stiffness degradation due to cracking. Fig. (7) depicts the FE patterns of cracking and crushing of concrete at the peak load. Through FE principal strain vectors, Fig. (8) helps to visualize the spread of loading in the zone surrounding the patch load.

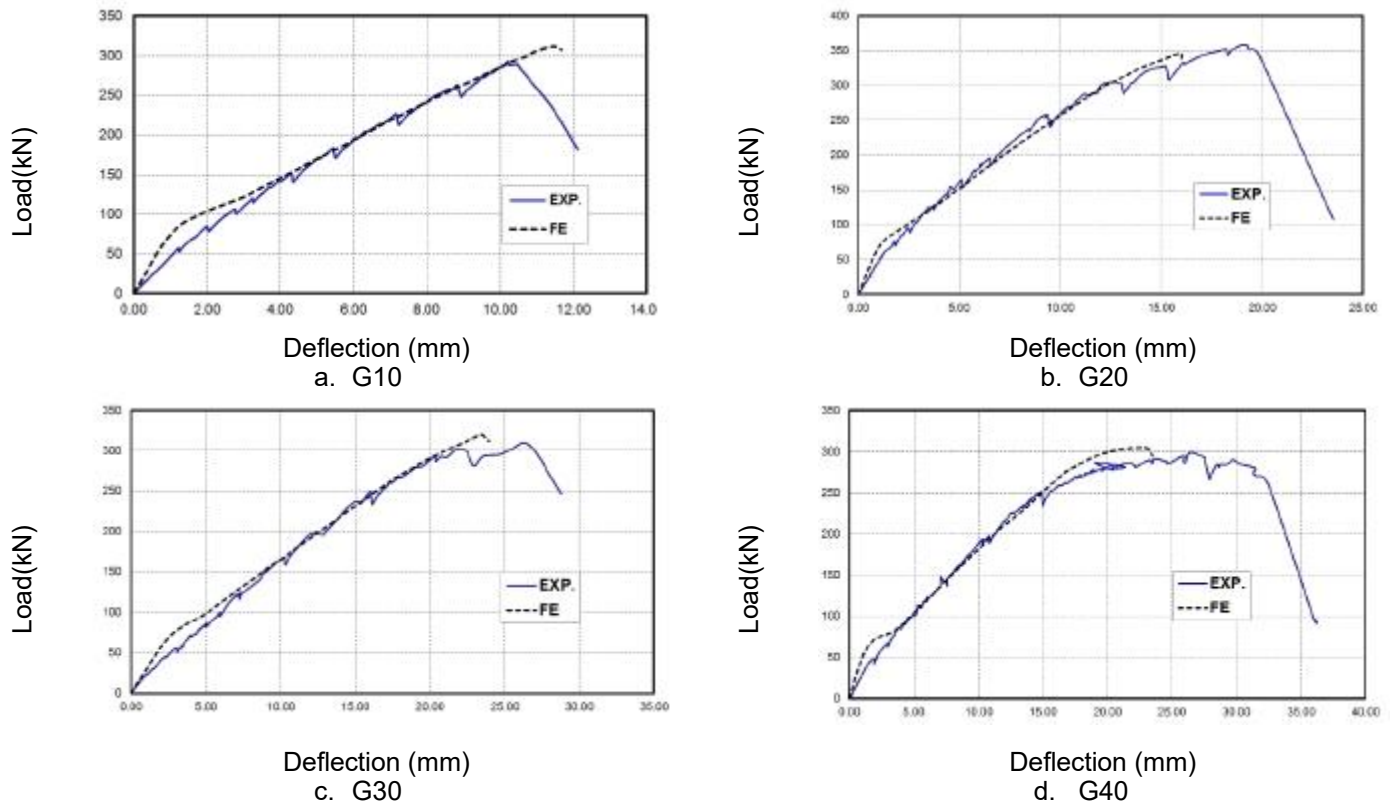


Fig. 6: Verification of the 3-D FE model against experimental observations.

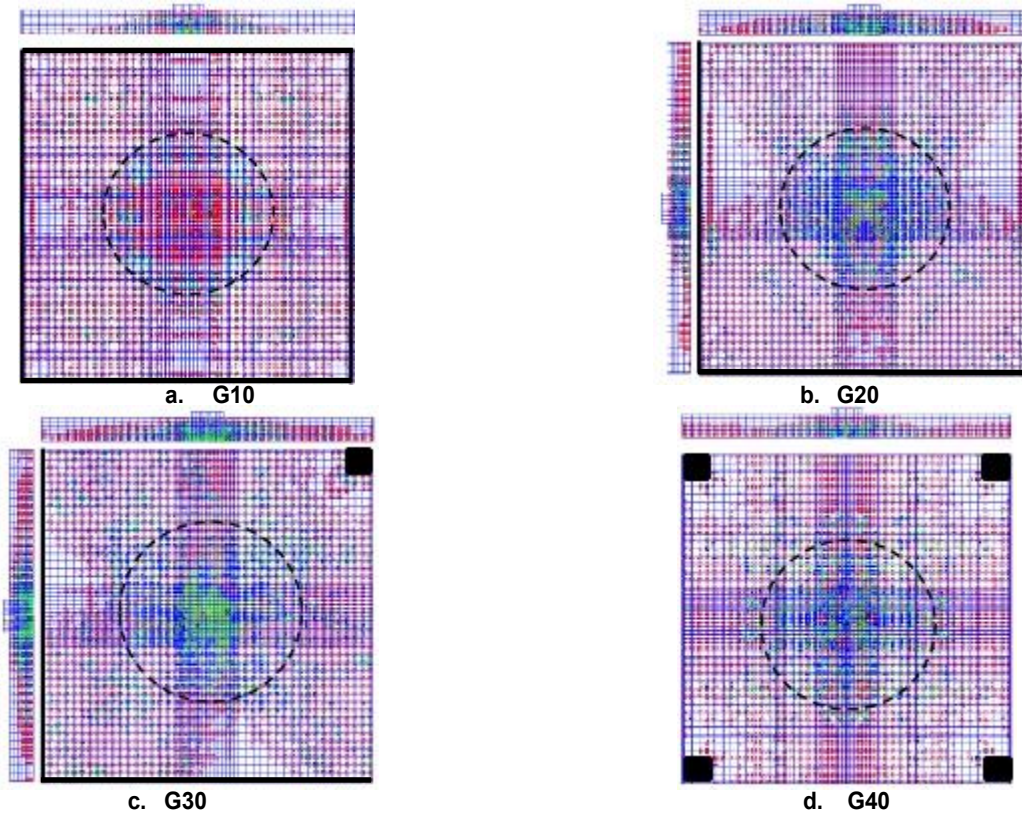


Fig. 7: Crack pattern at failure for verified specimens.



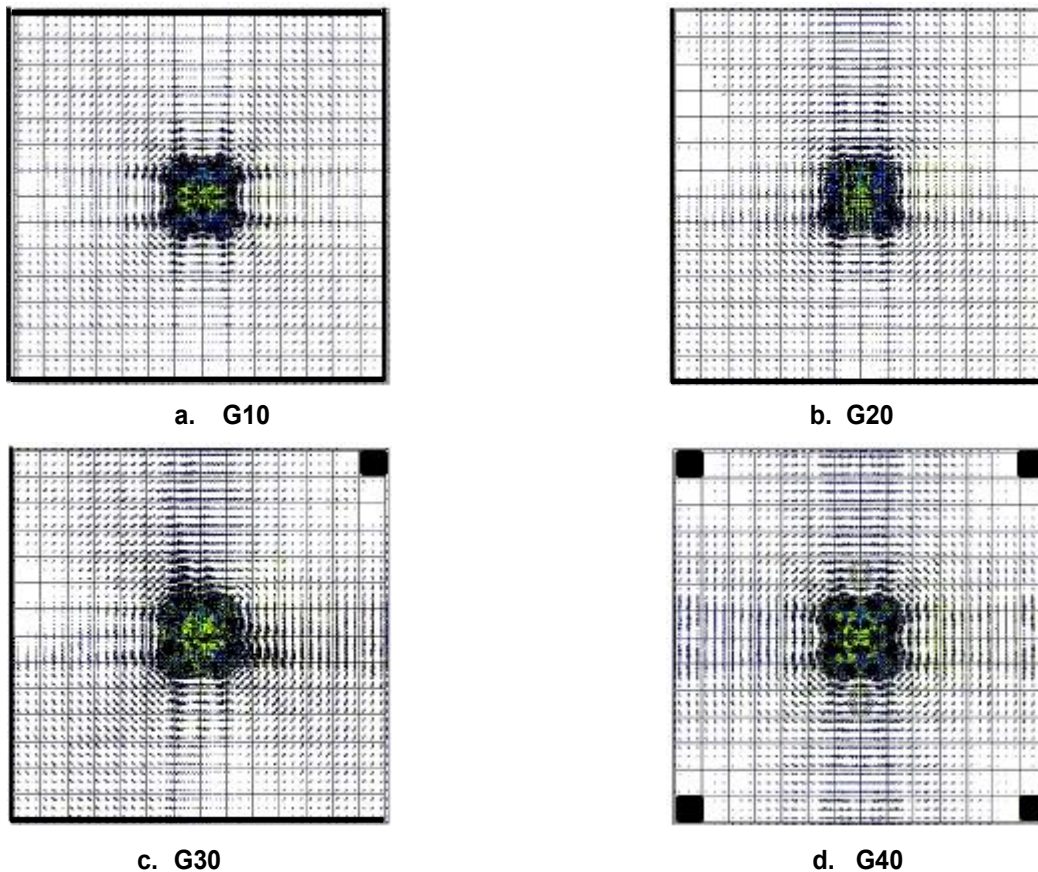


Fig. 8: Strain vector at failure for verified specimens.

## PARAMETRIC ANALYSIS

The parametric study presented hereafter, includes: i) the effect of reinforcement ratio of the tensile mesh ( $A_s$ ) along with presence of compression mesh along the whole span ( $A_s'$ ) and its ratio ( $\alpha=A_s'/A_s$ ), ii) the effect of limiting the length of the top mesh to particular length in the middle zone, iii) the effect of specimen size and iv) the effect of boundary condition.

For the first parameter, restraint group G1 was considered with bottom reinforcement meshes of variable rebars area. Fig. (9) presents the increase of the normalized punching capacity related to the Egyptian code prediction [37] with increasing the tensile steel mesh and by providing compression steel mesh. Of course, limitations of the minimum and maximum reinforcement ratios should be considered to avoid other brittle modes of failure. Asymptotic trend is reached at higher reinforcement ratio.

On the other hand for the second parameter, Fig. (10) indicates that spreading the top reinforcement mesh increasing the punching capacity. Actually the percentage increase for T16mm@120mm is only 7% for full span compression mesh over singly reinforced slab. Providing limited top reinforcement mesh under the patch load at four times the effective depth away from patch borders from each side is reasonable.

For the size effect, Fig. (11) shows the peak values of the FE runs for three sizes of RC slabs of the G1 group: i) normal size 1700mm side width, ii) half size 850mm side width and iii) double size 3400mm side width. The implication of changing the size is

altering the applied bending moment coefficient attributable to the punching load. Besides, the bottom reinforcement mesh was changed for each size similar to the first parameter. The main controlling parameter was found to be the ratio of the ultimate moment at failure to the nominal flexure capacity of the slab. This parameter implicitly involves the effect of all parameters constituting the nominal flexural capacity such as tensile reinforcement area, presence of compressive reinforcement mesh, effective depth and concrete grade.

For the fourth parameter, the boundary conditions G1, G2, G3 and G4 were considered with changing the tensile reinforcement mesh. Fig. (12) depicts the relationship obtained for the several case studies for the normalized punching shear capacity versus the ratio of the ultimate moment to the nominal flexural moment. The mathematical manipulation of the trend yielded best fit regression in a power form. This suggests modification of the punching capacity formula to be expressed as:

$$V_u = V_{UECP} \frac{M}{M}$$

This equation needs to be validate against numerous experimental data to have confidence in its application for practical purposes.

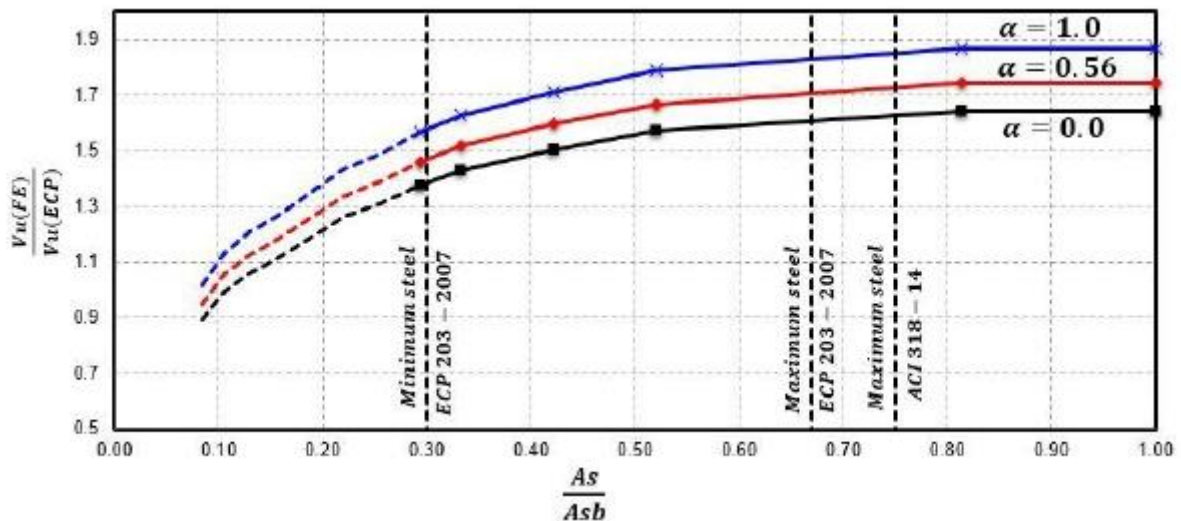


Fig. 9: Effect of steel mesh on punching failure load.

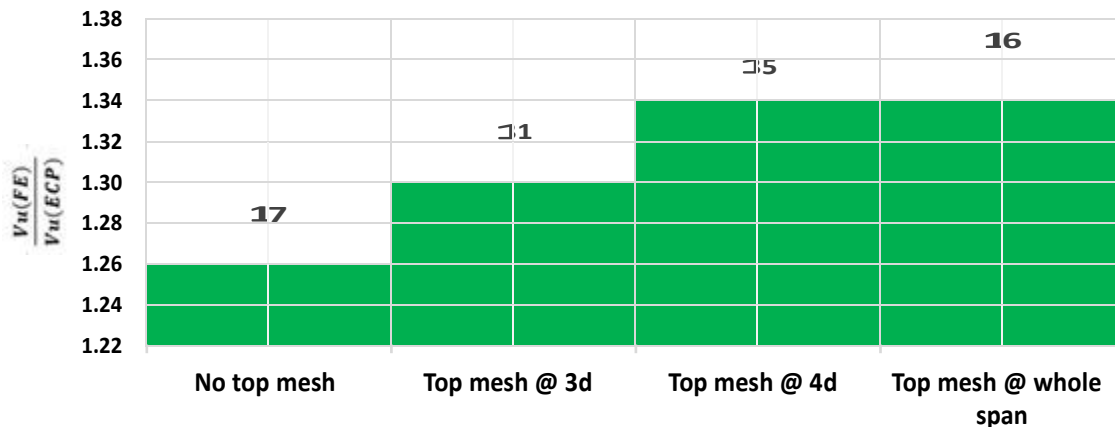


Fig. 10: Effect of full vs partial span compression steel mesh on punching failure load.

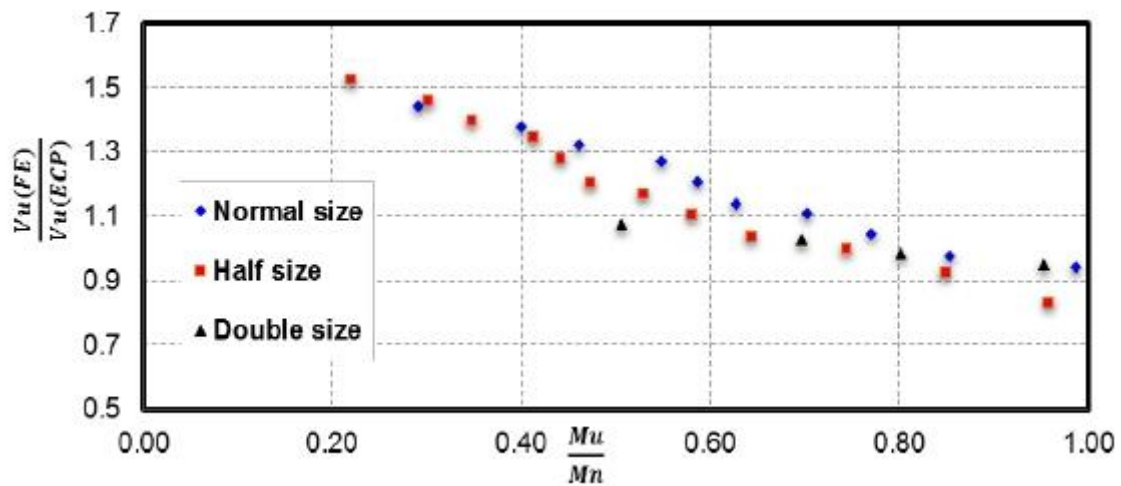


Fig. 11: Size effect of RC slab on the punching failure load.

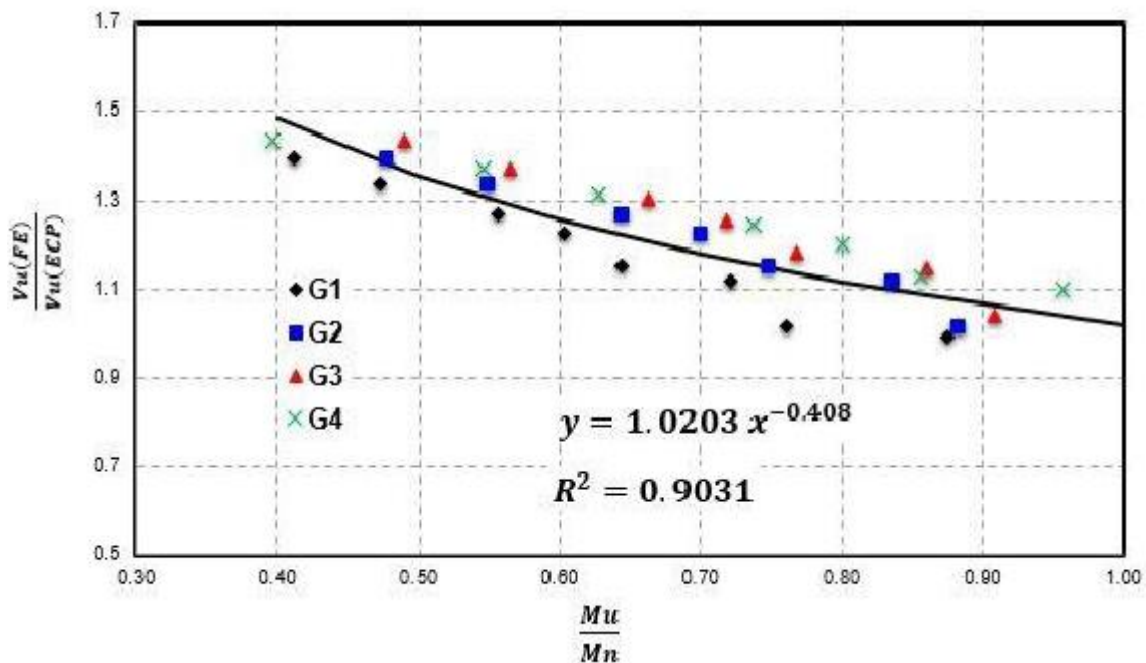


Fig. 12: Normalized flexural moment's ratio to punching loads ratio for case studies.

### AN OVERVIEW AND DISSCUSION

The global picture about the punching scenario, needs to be picked through numerous experimental tests. Reference [36] provided a great deal of information besides those reported in {5-35}. Using these data, Fig. (13) demonstrates the importance of not limiting the concrete punching capacity be a certain value as the trend is proportional for high strength concrete similar to ordinary strength concrete. In addition, the incorporation of the effect of reinforcement ratio should be implemented in predictions.

Validation of Equation (1) represents a practical approach to accept the idea of incorporating the combined effect of flexural moment with punching shear capacity. Fig.

(14) illustrates the very close agreement of the predicted capacity by the proposed equation with the experimental data of the more than 100 tests. The correlation coefficient is high which reflects the confidence of the proposed formula.

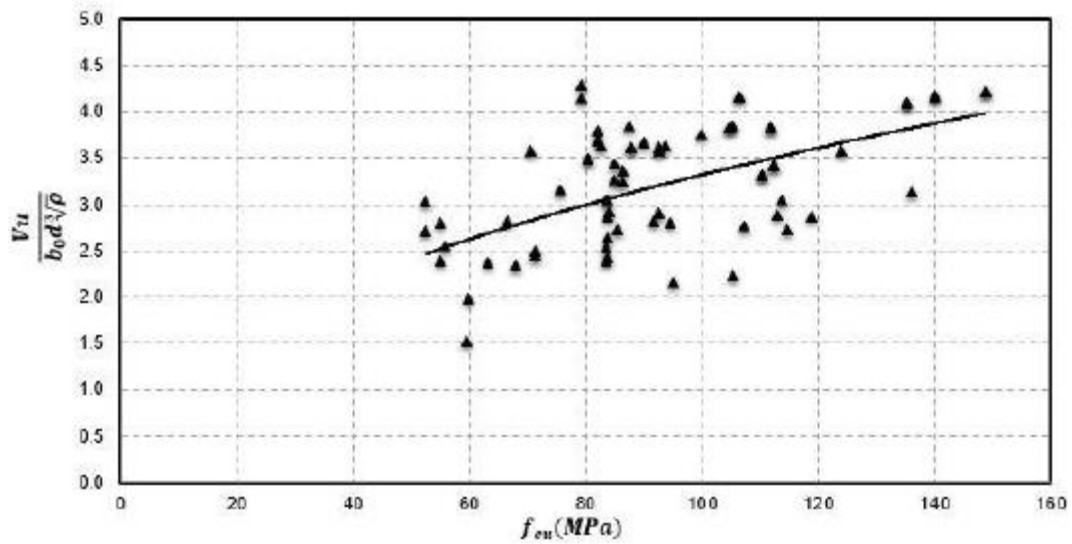


Fig. 13: Effect of concrete grade on the punching failure load [5-35].

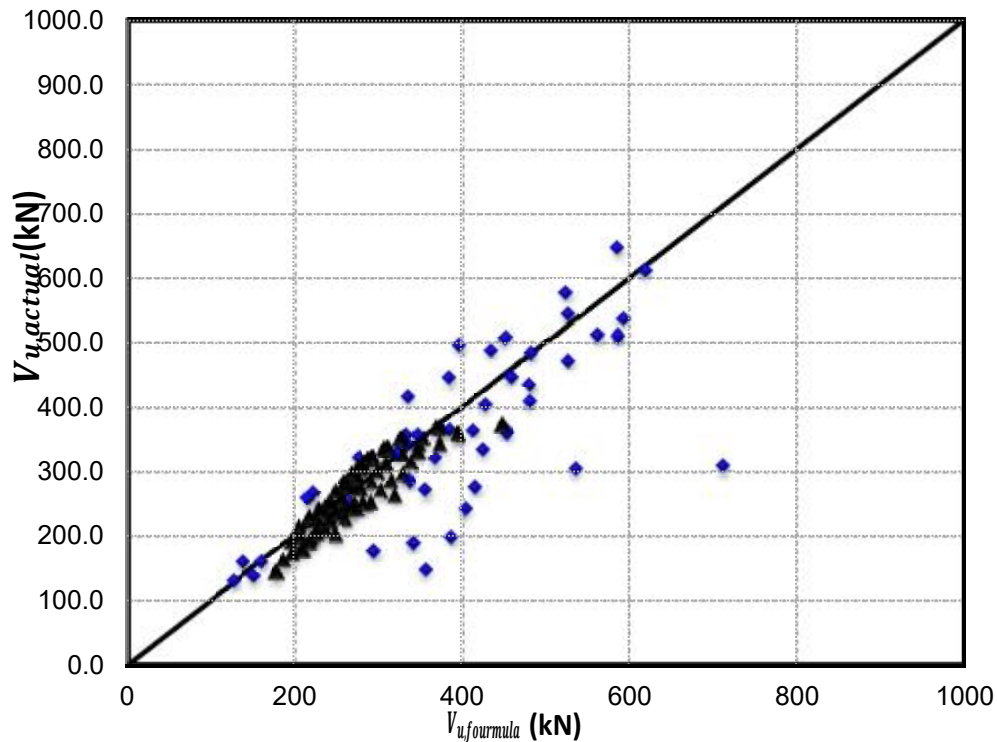


Fig. 14: Agreement of the proposed formula vs well-reported experimental data [5-35].

## CONCLUSION

From the exploratory experimental testing and the extensive finite element analysis and the comparison against numerous well-reported experimental data, the following conclusions may be drawn:

1. Changing the boundary conditions of the slab affects the induced bending moment due to patch loading that is associated with the onset of punching and thus influences the failure pattern.
2. Inclusion of short polypropylene fibers in the concrete mix enhanced the post punching behavior of the slabs and maintained relatively the integrity of the failed slabs.
3. For a particular flexural capacity, the bending moment induces cracking that reduces the effective thickness resisting the two way shear action. This effect is manifested by increasing the slab size.
4. The adopted nonlinear finite element models properly idealized the behavior up to the peak load as dowel action was not incorporated in the analysis.
5. Increasing the reinforcement area of the tensile mesh increases the ultimate punching load.
6. The gain in the punching shear capacity by providing top mesh in two way slabs is limited. However, top mesh underneath the patch load of length four times the effective depth away from patch borders from each side is reasonable.
7. The most controlling parameter for the influence of combined punching shear and flexural moment is the ratio of the ultimate moment to the nominal moment at the punching zone.
8. The proposed equation was validated against numerous well-reported experimental data that incorporates the combined effect of punching shear and the flexural moment.

## ACKNOWLEDGEMENTS

Thanks are due to the team of the Reinforced Concrete and Heavy Structures Laboratory at the Faculty of Engineering, Tanta University.

## REFERENCES

1. EL-Shafiey T. F., Hussein M., and Abdel-Aziz M. A., 2010, "Behaviour of Flat Slabs with Openings Adjacent to Columns", IACSG7.
2. Aoki.Y, Seki.H, 1974, "Shearing Strength and Flexural Cracking of Two-Way Slabs Subjected to Concentrated Load", Journal of the American Concrete Institute, ACI Special Pub. SP-30,103.
3. Ngo, D. T., 2001, "Punching Shear Resistance of High-Strength Concrete Slabs," Electronic Journal of Structural engineering, V. 1, No. 1, pp. 2-14.
4. Regan, P. E., 1986, "Symmetric Punching of Reinforced Concrete Slabs," Magazine of Concrete Research, V. 38, No. 136, Sep., pp 115-128.
5. Elstner, R. C., Hognestad, E., 1956, "Shearing Strength of Reinforced Concrete Slabs," Journal of the American Concrete Institute, ACI Proceedings, V. 53, No. 1, Jul., pp. 29-58.
6. Tomaszewicz A., 1993, " High Strength Concrete", SP2 –Plates and Shells, Report 2.3, "Punching oShear Capacity of Reinforced Concrete Slabs", Report #STF70A93082, SINTEF, Trondheim.
7. Gardner N. J., 1990, "Relationship of punching Shear Capacity of Reinforced Concrete Slab with Concrete Strength", ACI Struc. J., V.87, No. 1, pp. 66-71.
8. Hallgren M.and Kinnunen S., 1996, "Increase of Punching Shear Capacity by using High-Strength Concrete, 4<sup>th</sup> Int. Symp. On Utilization of High Strength/High Performance Concrete, Paris, pp. 1037-1046.

9. Metwally I. M., Issa M. S., El-Betar S. A., 2008, "Punching Shear Resistance of Normal and High-Strength Reinforced Concrete Plates", *ACI Struct. J.*, V. 94, No. 1, pp. 49-58
10. Marzouk H. and Hussein A., 1992, "Experimental Investigation on the Behavior of High-Strength Concrete Slabs", *ACI Struct. J.*, V. 88, pp. 701-713.
11. Marzouk H. and Jiang D., 1997, "Experimental Investigation on Shear Enhancement Types for High-Strength Concrete Plates", *ACI Struct. J.*, V. 94, No. 1, pp. 49-58.
12. Marzouk H., Emam M., Hilal M. S., 1998, "Effect of High-Strength Concrete Slab on the Behavior of Slab-Column Connections", *ACI Struct. J.*, V. 95, No. 3, pp. 227-237.
13. Adetifa B. and Polak M. A., 2005, "Retrofit of Slab Column Interior Connection using Shear Bolts", *ACI Struct. J.* V. 102, No. 2, pp. 268-274.
14. Abdel Hafez A. M., 2005, "Punching Shear Behavior of Normal and High Strength Concrete Slabs under Static Loading", *J. Eng. Sciences*, V. 33, No. 4, pp. 1215-1235.
15. Osman M., Marzouk H., Helmy S., 2000, "Behavior of High strength Lightweight Concrete Slabs under Punching Loads", *ACI Struct. J.*, V. 97, No. 3, pp. 492-498.
16. Ramdane K. E., 1996, "Punching Shear Strength of High Performance Concrete Slabs", 4<sup>th</sup> Int. Symp. On Utilization of High Strength/High Performance Concrete, Paris, pp. 1015-1026.
17. Fernández R. M., Mirzaei Y., Muttoni A., 2013, "Post-Punching Behavior of Flat Slabs," *ACI Structural Journal*, V. 110, USA, , pp. 801-812.
18. Moussa A., Ghanem G., and Tarkhan M. A., 2003, "Influence of Flexural Reinforcement on the Punching Shear Capacity of Reinforced Concrete Flat Slabs," Alexandria International Conference in structural and Geotechnical Eng., AICSCE5, Egypt, December.
19. Long, A. E., 1975, 'A Two-Phase Approach to the Prediction of Punching Strength of Slabs'. *Journal of the American Concrete Institute*, Proceedings, V. 72, No. 2, Feb., pp. 37-45.
20. Regan, P. E.; Bræstrup, M. W, 1985, "Punching Shear in Reinforced Concrete". *Comité Euro-International du Béton*, Bulletin, No. 168, Jan., 232 pp.
21. Kinnunen, S., Nylander, H., 1960, "Punching of Concrete Slabs Without Shear Reinforcement". *Transactions of the Royal Institute of Technology*, No. 158, Stockholm, Sweden, 112 pp.
22. Sherif, A. G.; Dilger, W. H., 2000, "Punching Failure of a Full Scale High Strength Concrete Flat Slab". *International Workshop on Punching Shear Capacity of RC Slabs – Proceedings*, Trita-Bkn Bulletin 57, Stockholm, Sweden, pp. 235-243.
23. Sherif, A. G.; Dilger, W. H., 2003, "Critical Review of Canadian Standards Association Standard CSA-A23.3-94 Provisions for Punching Shear Strength of Edge Column-Slab Connections", *Canadian J. Civ. Eng.*, V. 30, pp. 1069-1080.
24. Muttoni, A., 2008, "Punching Shear Strength of Reinforced Concrete Slabs without Transverse Reinforcement", *ACI Structural Journal*, V. 105, No. 4, July-Aug., pp. 440-450.
25. Wei, X., 2008, "Assessment of Real Loading Capacity of Concrete Slabs", MSc Thesis, Delft University of Technology, Delft, The Netherlands, 112 pp.
26. Hewitt, B. and Batchelor, B., 1975, "Punching Shear Strength of Restrained Slabs," *Journal of the Structural Division*, V. 101, No. 9, pp. 1837-1853.
27. Sherif, A.G, Emara, M.B, Ibrahim, A.H. and Magd, S.A., 2005, "Effect of the Column Dimensions on the Punching Shear Strength of Edge Column-Slab Connections," SP-232, Ed. Polak, M.A., American Concrete Institute, Farmington Hills, MI, pp. 175-192.
28. Csagoly, P. F., 1979, "Design of Thin Concrete Deck Slabs by the Ontario Highway Bridge Design Code, Ministry of Transportation and Communications", Ontario, 50 pp.
29. Moreno, J., "High-Performance Concrete: Economic Considerations," *Concrete International*, Vol. 20, No. 3, Mar
30. ASCE-ACI Committee 426, 1974, "The Shear Strength of Reinforced Concrete Members – Slabs," *Proceedings, ASCE*, V.100, No. ST8, pp. 1543-1591.
31. Collins, M.P. and Kuchma, D., 1999, "How Safe Are Our Large, Lightly Reinforced Concrete Beams, Slabs, and Footings?" *ACI Structural Journal*, V. 96, No. 4, pp. 482-490.
32. Mitchell, D., Cook, W.D. and Dilger, W., 2005, "Effects of size, Geometry and Material Properties on Punching Shear Resistance," SP-232, Ed. Polak, M.A., American Concrete Institute, Farmington Hills, MI, pp. 39-56.
33. Birkle, G., Dilger, W., 2008, "Influence of Slab Thickness on Punching Shear Strength," *ACI Structural Journal*, V. 105, No.2, pp. 180-188.

34. Taylor R. and Hayes B., 1965, "Some tests on the Effect of Edge Restraint on Punching Shear in Reinforced Concrete Slabs ", "Magazine of concrete research, V. 17, Issue.50, pp. 39-44.
35. Menetrey P., 2001, "Relationships between Flexural and Punching Failure" ACI structural Journal, V. 95, No.4, pp. 412-419.
36. Elsanadedy H.M., Al-Salloum Y. A., Alsayed S. H., 2013, "Prediction of Punching Shear Strength of HSC Interior Slab-Column Connections", KSCE Journal of Civil Engineering, V. 17, No. 2, pp 474-485.
37. Permanent Code Committee, 2007, Egyptian Code for Design and Execution of R.C Structures, ECP203.
38. ACI COMMITTEE 318, 2014, Building Code Requirements for Reinforced Concrete and Commentary", ACI 318-14, Farmington Hills, MI
39. EC2-1-1, 2014, Eurocode 2: Design of Concrete Structures-Part I: General Rules and Rules for Buildings,
40. British Standards Institution, 1997, Structural Use of Concrete, Part I: Code of Practice for Design and Construction, BS 8110-1, London, UK.
41. Canadian Standards Association (CSA): CSA A23-14, Design of Concrete Structures, Rexdale, Ont., 220 pp.
42. Dilger W., Elmasri M. Z. and Ghali A., 1978, "Flat Plates with Special Shear Reinforcement Subjected to Static and Dynamic Moment Transfer", ACI J. Proc., V. 75, Oct., pp. 543-549.
43. Smadi M. M., and Yasin, I. S. B., 2008, "Behavior of High-Strength Fibrous Concrete Slab-Column Connection under Gravity and Lateral Loads", Construction and Building Materials, Elsevier Publishing, V. 22, No. 8, pp 1863-1873.